Real-time state of charge estimation in thermal storage vessels applied to a smart polygeneration grid

M.L. Ferrari, A. Cuneo, M. Pascenti, A. Traverso
Thermochemical Power Group (TPG)
Dipartimento di Macchine, Sistemi Energetici e Trasporti (DIME)
University of Genoa, Italy

Contact author: Mario L. Ferrari (mario.ferrari@unige.it)

Abstract

In thermal grids and district heating, thermal storage devices play an important role to manage energy demand. Additionally, in smart polygeneration grids, thermal energy storage devices are essential to achieve high flexibility in energy demand management at relatively low cost. In this scenario, accurate evaluation of state of charge of storage vessels based on available measurements is critical.

The aim of this paper is to develop and compare three different models for state of charge estimation in stratified water tanks (discrete temperature measurements) and the related application in an experimental polygeneration grid with a real-time management tool. The first model is based on the empirical calculation of the state of charge considering the thermal power difference between generation and consumption, and afterwards correction based on measured temperatures. The second model is a mathematical approach considering a pre-defined temperature shape fitted with experimental data. The latter model is based on a 1-D physical approach using a multi-nodal method forced on the basis of the measured temperatures. The models were compared considering an experimental test performed in the polygeneration laboratory by the Thermochemical Power Group (TPG).

As a result of the comparative analysis, the first model was selected for applications in complex polygeneration grids, due to its good compromise between accuracy and computational effort. Several tests were carried out to demonstrate the performance of the empirical approach selected for the thermal storage model and the economic benefit related to the utilization of this vessel. The experimental plant, constituted by two different prime movers (a 100 kW microturbine and a 20 kW internal combustion engine) and a thermal storage tank, was able to demonstrate the performance of a real-time management tool. For this reason, special attention was devoted to the variable cost comparisons.

The novelty of this work lies in the development of the real-time management tool coupled with a thermal storage model by considering the simplified modelling approach. This is an essential requisite for complex polygeneration grids including hundreds or thousands of prime movers and thermal storage devices. Additionally, it is important to state that in such cases the required real-time performance could be difficult to obtain. The results, produced with the innovative and flexible experimental rig, demonstrate the positive impact of thermal storage as well as the effective management performance of this quite simple dispatching approach. Another important novel aspect regards this experimental assessment considering both specific 3-hour tests and extended conditions typical of a possible real application.

Keywords

Thermal storage; Smart grids; Vessel models; Experimental tests; Load demand management.

1. Introduction

Distributed generation facilities [1] are of increasing interest both at academic and industrial levels, owing to their potential benefits like cleaner production and cost effectiveness [2]. Special attention is devoted to the installation of small-scale power plants located close to the load [3] and connected to thermal grids, possibly arranged in smart polygeneration grids [4]. Energy generation in close proximity of the consumers is expected to reduce system outages [5], decrease risks of new grid investments [6], warrant the reliability and stability of energy supply [7] and reduce transport and conversion losses [8]. In addition, this technology plays a critical role in reducing the greenhouse gas emissions [9] through wide-ranging applications of small scale [10] high efficiency systems (e.g. fuel cell based plants [11]), cogeneration and trigeneration technologies [12] and renewable energy based plants [13].

Since these new polygeneration grids [14] can be equipped with several generators based on different technologies [15], the system management can be a demanding task. Moreover, each prime mover, considering also renewable source technology [16], has its own specific characteristics [17] in terms of design performance, off-design behaviour [18] and constraints (e.g. the start-up time and operational life cost). For this reason, an automatic tool [19] is essential to dispatch load demand, both electrical and thermal, to each generator according to cost effective algorithms [20]. Several management and optimization tools have been developed on the basis of different approaches (considering both traditional [21] and renewable sources [22] including the effects of climate conditions [23]) and verified at only simulation level [24]. Hence, experimental tests are essential to validate, tune and optimize these management algorithms (both control logics [25] for single systems [26] and optimization techniques for the entire grids [27]).

In this scenario, energy storage systems play an important role to improve the grid performance in terms of flexibility, efficiency increase and marginal cost decrease. Moreover, they can effectively compensate for non dispatchable renewable sources (mainly in case of solar, wind [28] and hydroelectric [29] energy). In thermal and polygeneration grids, thermal storage vessels are cost-effective solution to uncouple the electrical and thermal demands, contributing to avoid machine operations at low load and low performance conditions. Among different thermal energy storage approaches (e.g. phase changing materials, chemical storage devices, etc.), this paper focuses attention on hot water vessels due to the simplicity and straightforward integration with the thermal grids. Unlike the previous works on hot water vessels (for district heating [30] including renewable sources [31] or building issues [32]), in this paper special attention is devoted to real-time models for the state of charge estimation of the stored thermal energy: in fact, such models have to be simple enough for implementation in the plant acquisition/control system and to operate in real-time mode. Such tools have been used for the experimental tests performed in the smart polygeneration laboratory of the University of Genoa, Savona campus [27]. The experimental tests were essential not only to assess the vessel tools, but also to demonstrate the application in real plant management conditions, showing the benefit of thermal storage technology in smart grids managed by real-time tools, mainly in terms of marginal cost decrease.

In this paper, three different models to evaluate the state of charge (SoC) for thermal storage devices are presented, considering three different approaches: empirical (model n.1), mathematical (model n.2) and physical (model n.3). This modeling activity is essential because the actual temperature distribution is unknown (usually the vessel is equipped with a limited number of temperature sensors) and the management tools need to receive the storage SoC value in real-time mode as an input.

Additionally, management tests were carried out to demonstrate the reliability of the empirical model and the benefits related to thermal energy storage technology [27]. For these tests, a real-time management tool developed in Matlab®-Simulink® environment was used [33]. In comparison with previous works (considering both traditional [21] and renewable sources [22] including the effects of climate conditions [23]), these tests were carried out to demonstrate the real application of a simple management approach based on cost calculations: electrical and thermal loads are dispatched using a cost ranking of prime movers. Even if this tool (including a thermal storage management technique) was developed considering a quite simple approach, the results obtained in this experimental campaign have demonstrated its good economic performance, promising an effective scalability to larger scale polygeneration grids.

The important novel aspect of this work is the application of the real-time tool (including a simplified thermal storage model) in an experimental and flexible rig, which is capable to generate real operative conditions. While several previous works have presented offline management results with complete optimizers based on genetic or other complex algorithms, in this work a real online application is presented. The real-time performance and the reliability in plant management demonstrated in this work are essential aspects for polygeneration grids including hundreds or thousands of prime movers and thermal storage devices. In these cases, the novel simplified approaches for both the real-time tool and the vessel SoC calculation are able to maintain real-time performance differently from the complex algorithms.

2. Test rig description

The TPG installed an experimental rig (at Savona campus of the University of Genoa), which represents a laboratory scale smart polygeneration grid [33]. It is a test bench to develop, tune and demonstrate the management/optimization tools for distributed generation systems. This test rig (Fig.1-a) is composed of the following generators which are able to operate in cogeneration mode [18]: a 100 kW_e recuperated microturbine (T100 PHS Series) and a 20 kW_e internal combustion engine (TANDEM T20-A). Moreover, the facility is equipped with a 5 m^3 hot water tank able to store thermal energy.

Figure 1

Energy distribution is carried out with a direct connection to the campus electrical grid, and through an innovative two-ring thermal grid installed in the laboratory [33]: a hot ring operating at a nominal temperature of 75-80°C, and a cold ring at 50-55°C (Fig.1-b). While the hot water produced by the prime movers is collected by the hot ring, the cold one is receiving the return water flow from the users. As shown in [33], the ring temperature values are maintained almost constant by three-way valves installed for both generator and user devices. Each generator block is also equipped with a local fan cooler to emulate the building consumption, while a global fan cooler (shown in Fig.1-b) is also included to emulate the users directly connected to the grid and not able to generate thermal power. This component is connected to the rings as well as the generators, but it works with opposite flow (it receives hot water from the high temperature ring and delivers cold water to the other ring).

The possible thermal power mismatch between generation and utilization is compensated through the large vessel (5 m^3) connected between the rings (Fig.2 shows the storage tank with the location of temperature probes and the consequent division in zones) [27]. The bottom probe is located at 475 mm from the ground and the distance between two subsequent thermoresistances is 610 mm. In addition, this tank is essential for thermal energy storage in the form of stratified hot water. Thus, when consumption exceeds the production, the required heat can be obtained from water driven from the top of the storage tank to the hot ring. In the opposite case, hot water is supplied to the storage tank from the hot ring. Electricity supply/demand mismatches are simply managed by either purchasing from the grid, or selling the excess electricity produced to that same grid.

Figure 2

3. Thermal storage tank models

Since the accurate evaluation of SoC of energy storage systems [33] is fundamental for optimizing the plant management [34] also in case of renewable sources [35], this work shows three different tank models for a vessel which is able to store sensible heat in the form of hot water [36]. Three different modelling approaches were considered for different needs in terms of result accuracy, algorithm complexity and computational time (real-time performance [37] is a requirement, in this case).

3.1. Empirical approach (model n.1)

This model is based on temperature measurements coupled with thermal power difference between generation and consumption. Since the temperature distribution inside the vessel is stratified, it is possible to define a separation surface (or better a separation zone) between the charged part (at the generation temperature level) and the discharged one (at the return temperature value). Thus, the temperature sensors allow the calculation of the enthalpy value and the related SoC (Eq.1) for the vessel zones at high or low temperature levels. For the intermediate zone, in general, no accurate information is available from measurements, which are not continuous along the height. So, the thermal power difference of the connected devices is used with an integration approach (Eq.2 showing the enthalpy variation related to the Δt time). With Fig.2 reference, in case zones A, B and C are at the generation temperature level and zone E at the return temperature value, the procedure necessary to evaluate the enthalpy and SoC values in the intermediate zone is applied to "Zone D".

$$SoC = \frac{H}{H_{\max}} \cdot 100 \tag{1}$$

$$\Delta H_{storage} = \int_t^{t+\Delta t} \Delta P_{th} \cdot dt \tag{2}$$

Since this approach is significantly affected by thermal losses and measurement errors, it is necessary to compensate the model by introducing an empirical loss value. It is calculated in real-time mode on the basis of the temperature difference between the water content and the ambient and the external surfaces of the storage vessel and the pipes. This compensation is essential to avoid significant errors during long time tests [33]. However, due to uncertainties in such calculation, the model includes a further approach to align the SoC value with the temperature measurements. In the intermediate zone, the integral result is forced to match the calculation carried out with the measured temperatures when one of the two temperature probes (located on the top and on the bottom of the intermediate zone) reaches the high or the low temperature value. Since the exact matching with the temperature set-point is a rare case (due to thermal losses), a tolerance band of ±3°C is necessary. In case the hot ring set-point would be 75°C, during a charging phase the integral is forced to match the enthalpy calculation based on the measured temperatures when the temperature sensor at the top of the intermediate zone reaches 72°C. Moreover, to avoid discontinuous behaviour between the fully charged or discharged parts and the intermediate zone, a linear temperature variation was introduced for the connection between the zones.

3.2. Mathematical approach (model n.2)

The aim of this model is the calculation of the enthalpy for the water stored into a vessel (and the related SoC value) using a hypothetical temperature curve that fits the real temperature distribution acquired via field measurements. Remarkably, this model does not need mass flow and thermal flow measurements.

Two main hypotheses were considered to build this model: temperature distribution along the vessel sections is a continuous function of section heights, and temperatures are constant within a defined vessel section. This second hypothesis is applicable when the convective motions are negligible (stratification conditions) and the flow velocity inside the vessel is low. Based on such hypotheses, it is possible to build a mono-dimensional temperature function, which is dependent only on the height (z) of the vessel. Through this function, the stored enthalpy can be calculated. The needed function must always be continuous, increasing and symmetric with a concavity change into mirror plane only, with two real limits at ±∞ very close to the maximum and minimum temperatures of the vessel. The Eq.3 which is suitable to fit the experimental data with good accuracy, shows the vessel temperature in relation of height level (z) on the basis of 5 parameters (a, b, c, d, e) calculated with a fitting tool named Constrained Nonlinear Curve Fit LM Bounded [38]. It fits a curve using a "first try" set of parameters into a Levenberg-Marquardt algorithm. Furthermore, the resultant parameters are coerced into a defined bound, to ensure the physical plausibility of the solution.

$$T(z) = \frac{e \cdot (d \cdot z - a)}{\sqrt{c + (d \cdot z - a)^2}} \ln \sqrt{c + (d \cdot z - a)^2} + b \qquad (3)$$

By changing the parameter a,b,c,d, and e, it is possible to change the curve to adapt it to the measurements. Figure 3 shows this function with the following parameter values: a=130, b=65, c=d=1, and e=2.1. It is a plausible trend of the temperature in a real 5 m^3 tank.

Figure 3

Curve fitting needs at least five temperatures to obtain univocal solution from the fitting process. So, the volume inlet and outlet temperatures can also be used. This choice is acceptable when the mass flow rates are not negligible, which is verified in the experimental set-up under investigation (hot and cold tubes feeding at the extremes of the vessel). In case of low mass flow rates, an apt weighting process of the inlet and outlet temperatures has to be implemented, to keep into account the temperature deviations due to thermal losses.

The component is modelled like a stack of one-centimetre high elemental volume where temperature (calculated with Eq.3) is considered constant for all its internal points. On the basis of these calculations, the vessel enthalpy is calculated as the sum of enthalpy of each elemental volume.

3.3. Physical approach (model n.3)

In this case, the thermal storage tank has been modelled with a multi-nodal method, based on a numerical 1D finite difference scheme. It consists of dividing the vessel in N sections (nodes) and solving an energy balance for each of them. Thus, a set of N differential equations is used to obtain the temperatures of the N nodes as a function of time. The problem domain was divided into N parts, spatially distributed in the z direction (Eq.4).

$$\Delta z = \frac{H}{N-1} \tag{4}$$

N is the number of nodes predetermined by the user. It is a fundamental parameter of the system, since it defines the model accuracy. H is the height of the tank. In this way, the whole storage is subdivided into N portions of water, each having the ith mass (Eq.5).

$$m_i = \rho_i A_i \Delta z \tag{5}$$

The temperatures of these N masses are the outputs of the problem. Therefore, there are N unknown values to be calculated at each time step. To solve the mathematical problem, N differential equations are used, linking the temperatures with the model parameters, as well as taking into account the following different internal and external phenomena:

- heat conduction between the various water masses;
- heat losses between the masses and the outside;
- inlet or outlet water flow rate (positive or negative);
- internal natural convection .

Figure 4 shows the tank scheme discretized into N parts.

Figure 4

The energy balance considering different internal and external phenomena is reported in Eq.6.

$$\frac{(\rho \cdot v \cdot A \cdot \Delta z)}{2} \cdot \frac{dT_i}{dt} = q_{c,i} - q_{conv,i} + q_{s,i} + q_{m,i} \tag{6}$$

The mathematical time-dependent integration is performed through the implicit Crank-Nicolson method.

The most important parameter associated with the heat storage is the enthalpy content of the stored water (SoC parameter). The estimation of this parameter is affected by an error that increases with the decrease of the number of temperature nodes, because the theoretical exact value of the SoC could be obtained only with N tending to infinite. The objective is to improve the estimation accuracy of the stored heat amount (typical problem of system state identification) with a limited number of nodes, and taking advantage of the field measurements. Conventionally, this estimation is performed indirectly through the detection of temperatures at various heights of the tank: the thermal stratification of water and the small number of sensors involve estimation errors in enthalpy calculation. Figure 5 shows an example of the errors related to the State of charge (SoC) evaluation (Eq.1) for a thermal storage vessel. With this approach errors higher than 25% may occur.

Figure 5

It is clear that reducing temperature measurements (number of nodes) the error increases; for example, the difference in SoC value that is estimated using 2 temperatures instead of 8 is 24.6%. The model implementation was carried out in Matlab-Simulink environment. The measurements of thermoresistances (four probes in the laboratory test case) were forced at the related i-th node, to take the advantage of experimental evidence: in such respect, the model can be regarded as a tool to physically interpolate between the temperature measurements. This approach is essential to avoid significant error accumulation and increase over time. While in calculation models errors under 1-2% are considered acceptable, in the thermal storage case such difference in SoC evaluation could generate errors higher that 30-50% after several hours of operation (as typically carried out for these systems). Thus, the temperature forcing approach is able to compensate the errors on the basis of actual measurements. The model has to estimate the remaining temperatures: these temperatures will be used for a more accurate estimation [39] of the SoC value of the vessel.

4. Results of thermal storage tank models

This work shows a test carried out on the 5 m^3 tank related to both charging and discharging phases. The initial charging level condition was 72% of its maximum. During the initial 17000 s, the thermal power difference between generation and consumption was close to zero. Subsequently, the machines were managed to have an excess of thermal utilization (average value: about 51 kWth) followed by a generation value significantly higher than the consumption (average value: about 38 kWth). As already explained in a previous work [27], the enthalpy (and the consequent SoC) was calculated considering 55°C as reference temperature (i.e. stored enthalpy is 0 MJ (SoC=0%) with the tank temperatures uniform at 55°C). This reference value was chosen because the temperature set-point of the cold ring was fixed at 55°C (this means that during operations, excluding the grid start-up phase, 55°C is the lowest temperature value in the vessel). The main results obtained with all the models are shown in Fig.6: almost constant SoC value in the initial part, followed by a sensible decrease and a final increase.

4.1. Comparison

Since no experimental data are available for the SoC, and these models were developed really to evaluate a property that cannot be measured or easily obtained from the available measurements, an assessment of model performance is shown here considering the general SoC trend. In details, a continuous trend is better representing the real phenomena, while an SoC curve with spikes or instantaneous trend changes is considered less accurate.

Since the Model n.1 is based on the simplest approach (thermal power difference between generation and consumption), it can also be considered as the reference case. However, to compensate a possible significant error accumulation, the correction based on the measured temperature values generates some discontinuities (5% order of magnitude) in correspondence of compensation zones. They are visible in Fig.6 close to 20000 s, in the trend inversion zone and close to 25000 s. Model n.2 shows more discontinuous behaviour due to temperature fitting problems and to rapid fluctuations of inlet/outlet temperatures. The Model n.3 is in good agreement with the results obtained with the Model n.1. It produces a more continuous trend because it is based on a physical approach, able to compensate thermal losses and power measurement errors with good accuracy. In this case, the matching with the measured temperatures is carried out during the entire model operations, instead of in specific conditions (as in the other models). Even if the Model n.3 seems to be the most reliable solution for its continuous trend, both simplified approaches (empirical and mathematical) can be used for management of polygeneration grids. This aspect is very important in case short calculation time is necessary (e.g. in complex large grids).

Figure 6

To conclude this discussion, Fig.7 shows the temperature distribution calculated with the Model n.3 and the temperature measurements obtained with the probes installed in the vessel (T_1, T_2, T_3 and T_4). These measured values (the bold lines in Fig.7) are the same for all the models because they are used to evaluate the vessel state of charge related to the same experimental test. The significant temperature decrease/increase due to the discharging/charging operation is shown by both measurements and calculated values. The inversion of temperature trends (shown by T_1 at about 22000 s after the test beginning) is in agreement with the time of the lowest value in the plot related to the SoC.

Since the measured temperatures are input data for the model, they are exactly matching the temperature values of the related calculation node. So, these measured temperatures cannot be used for model validation. The only model assessment can be carried out considering the temperature distribution obtained between the measured values and the related continuous trend, as discussed for the SoC value in Fig.6.

Figure 7

5. Real-time tool for smart grid management

The application and the related importance of thermal storage tank models were assessed by the laboratory tests carried out with a real-time management tool which is capable to perform a market-oriented control strategy on the prime movers. So, even if it is not based on a rigorous complete optimization approach, it is a simplified tool developed to perform an economic improvement of prime mover management. Considering a marginal cost ranking (including profit too) related to all the prime movers, the tool (implemented in Matlab-Simulink environment) performs a control action [27] on the electrical set-point values to reduce the generation costs. This ranking is calculated in real-time mode on the basis of the specific measurements acquired continuously and, as a consequence, taking into account the prime mover off-design performance. So, in case of a thermal energy overproduction, the tool applies a set-point decrease on the most expensive prime mover, while in the opposite case (i.e. a thermal demand increase), the software generates a ramp-up operation for the less expensive generator. The tool is able to switch on/off the machines, if necessary, to decrease the generation marginal costs and to take into account different constraints (e.g. maximum/minimum generation power values, maximum acceptable set-point slopes and waiting times for machine switching on/off, etc.). As previously described in [27], even if this is not a real rigorous optimizer, this is a very simple and modular approach able to operate in real-time mode in complex smart grids equipped with a very large number of prime movers.

The thermal storage tank management is included in the general tool considering historical data (the tool stores data related to demand/generation profiles and tank SoC value) on the basis of a management period (even if each period usually corresponds to 24 hours, it is possible to consider shorter time range for test reasons). Using these stored data the tool calculates (considering costs, maximum acceptable values and profits) the engine constraints (P_{upper_limit} and P_{lower_limit}), thus generating an operative range where the thermal demand can be uncoupled from the generation using the storage vessel. During low thermal demand conditions, the prime movers can be ramped down (switched off too) or maintained at high load values generating electricity for the grid and charging the thermal storage tank. The stored amount has to be used to cover thermal demand peaks occurring especially during low electrical demand conditions. The tool calculates the P_{upper_limit} value to satisfy Eq.7. Stating the need to obtain a significant amount of historical data updated period by period, this software is able to effectively manage the storage tank starting from the third period. Even if the typical period duration is 24 h, shorter duration values are possible for laboratory test reasons.

$$\begin{cases} P_{demand}(t) \geq P_{upper\_limit}(t) \\ \int_0^{period\,lenght} \left(P_{demand}(t) - P_{upper\_limit}(t)\right) dt = E_{Sto\,upper\_limit} - E_{Sto\,lower\_limit} \end{cases} \quad (7)$$

$E_{Sto\,upper/lower\_limit}$ are calculated constraints considering technical and empirical evaluations.

Moreover, with a similar procedure, the P_{lower_limit} is calculated with the following equations (Eq.8).

$$\begin{cases} P_{demand}(t) \leq P_{lower\_limit}(t) \\ \int_0^{period\,lenght} \left(P_{lower\_limit}(t) - P_{demand}(t)\right) dt = E_{Sto\,upper\_limit} - E_{Sto\,lower\_limit} \end{cases} \quad (8)$$

In case the values are not able to satisfy the first conditions of Eqs.7 and 8, the power limit values are reset to fixed constraints.

6. Polygeneration grid management tests

This section shows the experimental tests carried out with the laboratory rig managed by the real-time tool presented in the previous section. The results obtained without the management of the thermal energy storage tank (the vessel was included in the rig, but the SoC set-point value was maintained constant) are compared with the same performance parameters obtained with the algorithm presented for the storage tank in the previous section. In both cases, the same demand values (for both electrical and thermal power) were used during the tests. For laboratory constraints related to the test duration, a 3-hour period was considered. This approach was necessary to perform each test during a reasonable time (12 hours) because further three hours are necessary to pre-heat the rig, and the tests with the storage tank management require the repetition of at least 3 periods. However, this approach can demonstrate the tool performance in perspective of applications to real systems (with 24-hour periods). The power demand data considered for these 3-hour period tests are shown in Fig.8, where both electrical and thermal values are reported for all the users. Since each generator block is able to emulate a building equipped with a prime mover and energy consumption devices (responsible of electrical and thermal local demands), Fig.8 shows the different demands for each user (as mentioned in section 2, while electrical demands are generated just with the machine connected with the laboratory electrical grid, the thermal demands are generated with fan coolers located in the generator blocks or at the thermal grid level). The temperature set-point values for the thermal grid were set to 75°C and 55°C for the hot and return ring, respectively. So, the end users are receiving water at 75°C nominal value (the thermal losses can result in 0.2°C maximum temperature decay from the nominal value). The demand data shown in Fig.8 were defined to highlight the tool skills considering the management of case-limit conditions. For this reason, some demand curves were defined taking into account a completely decoupled situation between electrical and thermal peaks. Although they are not representative of a typical district, they allow highlighting the tool performance in a short time period considering a challenging scenario. The emulated building equipped by a specific prime mover can have a demand higher than the maximum power that can be generated by it. This is possible because the excess power can be supplied by another emulated building, by the grid (for the electrical demand) or by the thermal storage vessel (for the thermal demand). In the input data shown in Fig.8, the excess of electrical power demanded by the emulated building including the ICE has to be covered by the microturbine or by the electrical grid, as managed by the real-time tool.

Figure 8

The tests discussed here were started under the following conditions: ICE at maximum load (20 kW) and mGT at about 39.5 kW electrical power (in case of thermal storage tank management, the test starts with mGT at 52.2 kW because in this case the results are related to the third period). Since no ambient temperature control can be performed, during these tests this parameter was in the 15-23°C range. Additionally, the following data were used as an input for the management tool, considering countries which are affected by high energy costs at household level (e.g. the situation in Italy in 2015):

- Fuel price: 0.091 €/kWh [40]
- Electricity price (purchased from the grid): 0.24 €/kWh [41]
- Electricity price (sold to the grid): -0.11 €/kWh [27]

In the tests shown in the following sub-sections the SoC value of the thermal storage tank was evaluated using the Empirical approach (model n.1). Moreover, a comparison with the Physical approach (model n.3) is presented in section 6.4 to further demonstrate the reliability of model n.1 for applications in complex polygeneration grids.

Since the SoC at the end of the test can be significantly different from its value at the beginning, it is necessary to include the cost related to this missing/additional energy in the global cost evaluation. To consider the possible worst condition, this additional cost was calculated in all the following tests by considering a standard boiler (90% efficiency) operating with natural gas.

In the final subsection (6.5) an extended test carried out with the real-time management tool is included, to shows the results related to conditions typical of real applications.

6.1. No management of the thermal storage tank

The results obtained with the rig managed by the tool without operations on the thermal storage tank are shown in Fig.9. The thermal storage tank was not excluded from the test rig, but it was simply maintained at fixed SoC set-point (67%). For this reason, the tank participates to compensate the small power mismatches (due to components control system delays) as shown in Fig.9 by the slight differences between demand and generation in total power values and the consequent SoC oscillation (in the ±15 MJ range). So, the total thermal generation (±3.5% average accuracy considering the sum of ICE and mGT thermal power) followed the total thermal demand (thermal energy consumption caused by the fan coolers) affected by ±4.3% average accuracy (the sum of thermal power consumed by mGT, ICE and grid fan coolers). The total fuel consumed during this 3-hour test was 63.09 kg responsible of 76.55 € cost. Moreover, additional fuel (0.08 kg) producing 0.11 € further cost, has to be taken into account to compensate the slight SoC decrease. Moreover, since 0.87 € cost has to be considered for the electrical balance (105.26 kWh sold to the grid at 0.11 €/kWh and 51.86 kWh purchased from the grid at 0.24 €/kWh), the total marginal costs of this test was 77.53 €, on the basis of a global balance related to the whole polygeneration system.

These results obtained with this real-time tool without operations on the thermal storage tank can be compared to results related to traditional standard management of the prime movers (the ICE managed to satisfy its local thermal demand and the mGT operated on the rest of the thermal demand). In this standard approach, the ICE was not at maximum load for a large part of the test due to low demand range of 15-37 kW range (see Fig.8) implying a significant electrical efficiency decay [18]. As mentioned for the management tool description, the efficiency decay in part-load conditions was taken into account because it was calculated in real-time mode on the basis of the fuel mass flow rate and the generated power. So, the total cost (global balance) in this standard case was 86.36 € for a fuel consumption of 71.95 kg (87.30 € cost) and an income related to the electrical energy balance equal to 0.94 € (100.15 kWh sold to the grid and 41.97 kWh purchased). In conclusion, this comparison between the test based on the real-time tool with a standard management case showed a 10.2% cost decrease thanks to the software application.

Figure 9

6.2. Management of the thermal storage tank

Figure 10 shows the results obtained with the real-time tool including the management algorithm for the thermal energy storage tank. On the basis of the historical data (this was a third period operated immediately after two former periods with the same demand values), the tool maintains the ICE at maximum load and the mGT at almost constant set-point value (calculated on the basis of the algorithm presented in the previous section). So, the storage tank was discharged during the initial 5400 s (high thermal demand condition), and recharged during the second part of the test affected by low thermal demand values. As shown in Fig.10 the SoC line is affected by some slight discontinuities due to the characteristics of model n.1. However, the results show that these aspects are not limiting the model performance, because it is able to well operate for such kinds of polygeneration grid management. The total fuel consumed during this test based on the storage tank management was 65.25 kg generating 79.17 € cost. However, since the final SoC value is higher than the initial one, the fuel amount (0.32 kg) and the related cost (0.44 €) has to be subtracted because of the energy available in the storage tank. Moreover, the electrical balance generated 7.51 € income due to 79.07 kWh sold to the grid and 4.94 kWh purchased from the grid. So, the total cost calculated for this test was 71.22 € on the basis of a global balance related to the whole polygeneration system. In conclusion, comparing these final results with the test performed without the management of this energy storage component, it is possible to highlight 8.1% cost saving obtained with the management of the storage tank.

Figure 10

6.3. Result comparison

Figure 11 shows the total marginal costs evaluated for each case. Thanks to a 17.5% cost decrease obtained with the test carried out with the real-time tool including the thermal storage tank management (in comparison with the standard case), it is possible to demonstrate the effective performance of this management tool. Therefore, this real-time tool, based on a very simple management algorithm and equipped with a very simple SoC calculation model (model n.1 presented in section 3 and validated in section 4), has demonstrated its ability to obtain a significant improvement in polygeneration grids. This is an important result especially for the management of complex grids (high number of generators and thermal storage tanks), where complex modelling and optimization techniques could not be acceptable.

Figure 11

Table 1

A sensitivity analysis was also carried out to show the effect of different electricity prices. Since the Italian case is affected by high electricity prices, results considering different scenarios were calculated to extend this analysis to other countries with lower prices for electrical energy. The main economic results are shown in Tab.1 considering the comparison of tests carried out either with the real-time tool enabled to manage the thermal storage vessel or operating at constant SoC set-point. While the economic benefit related to the thermal storage management was higher at high electricity cost conditions, also at low unitary electrical costs the tests carried out with the vessel management produced lower marginal costs (fuel price was constant in all cases).

Table 2

To complete the cost sensitivity analysis for the 3-hour tests, Tab.2 shows the effect of different fuel prices considering possible countries with lower costs. For this analysis the electricity prices were maintained constant: 0.24 €/kWh for energy purchased from the grid and -0.11 €/kWh for the energy sold to the grid. Also in the cases reported in Tab.2, the results are able to show the significant benefit of the vessel management in comparison with the results obtained without enabling this option in the real-time tool.

6.4. Impact of storage model type on management results

To evaluate the impact of storage model on these management results, the same 3-hour test was carried out also with the model n.3 for the SoC calculation. While the ICE was at maximum load for the entire test, attention on Fig.12 is focused on the properties showing trend modifications in comparison with the Fig.10 results. For this reason, the values obtained for the SoC, mGT electrical power and total generated thermal power are reported and compared with results obtained with model n.1. Figure 12 shows that the most complex and reliable storage model generated a more continuous trend in the SoC curve. However, the difference in the calculated values is not exceeding 5% of the full charged condition during the entire test. The marginal cost calculation related to the fuel consumption and the electrical energy balance with the grid was carried out considering the Italian scenario for the year 2015. The total mass of fuel consumed during this test (storage tank management with SoC calculation carried out with the model n.3) was 64.93 kg generating 78.78 € cost. However, since the final SoC value is higher than the initial one, a fuel amount (0.20 kg) and the related cost (0.27 €) has to be subtracted (energy available in the storage tank). Moreover, since the electrical balance generated 7.06 € income, the total cost calculated for this test was 71.45 €, on the basis of a global balance related to the whole polygeneration system. While the global results are very similar (0.3% increase in global costs) to the data obtained using model n.1, the test is a further demonstration of the simplified approach capabilities. So, model n.1 is a good solution for the management of complex rigs or districts, considering that errors in global cost calculation are significantly lower than errors due to measurement accuracy.

Figure 12

6.5. Application to an extended test

To complete the evaluation of the real-time tool performance, the results of a long time test are presented. Also in this case the SoC value for the storage tank was calculated with the model n.1, due to the good compromise between simplicity, result reliability, and possible application in complex grids. The demand values shown in Fig.13 were related to an operation period between 8:00 a.m. to 5:00 p.m., as in a typical district related to daytime activities (e.g. office work). The test was not related to the complete campus demand, but a specific fraction selected for the tool assessment. Unfortunately, due to a real demand value higher than the machine sizes, an operation with the entire campus demand is not significant for the comparison with a standard case. In both cases, the machines have to be at maximum load for the entire test.

Figure 13

Figure 14

Figure 14 shows the results obtained during this test managed with the real-time tool. Since during the initial 3 hours the operations are carried out to obtain enough historical data for the SoC management, the machines almost matched the thermal demand. Then, during the following hours the tool managed the thermal vessel with a significant discharge operation.

The effectiveness of the tool is shown in Fig.15, where the operation cost of this extended test (machines managed by the real-time tool) is compared with a standard approach (the ICE managed to satisfy its local thermal demand and the mGT operated on the rest of this thermal demand). Since in this case, the SoC at the end of the test is significantly lower than its value at the beginning, it is necessary to include the cost related to this missing energy in the comparison with the standard case. This was considered to calculate the cost for the additional fuel (6.13 kg) necessary to compensate this SoC decrease (70.4%).

The total mass of fuel consumed during this extended test was 180.57 kg generating 219.09 € cost. Moreover, the electrical balance generated 2.35 € income due to 207.93 kWh sold to the grid and 85.52 kWh purchased from the grid. So, the total cost calculated for this test was 225.01 € on the basis of a global balance related to the whole polygeneration system and including 8.27 € additional cost for the mentioned SoC vessel decay. In conclusion, comparing these final results with the reference case test (Fig.15), it is possible to highlight a 13.3% cost saving obtained with the real-time management tool.

Figure 15

Comparing the results of this extended test with the 3-hour case, it is possible to highlight that the cost saving percentage is dependent on the demand curves. Considering the standard case, it is possible to obtain a cost saving in the 0-20% range with operations including the thermal vessel management. In details, no cost saving is present in case of constant demand values equal to the nominal machine loads (both electrical and thermal generation), because in both cases (operations with the real-time tool or with the standard approach) the machines have to operate at maximum power condition. In case of lower demand values showing oscillations, it is possible to have a significant benefit (up to 10-20% cost saving performance) especially in case of large application of thermal storage vessels. The paper demonstrated 17.5% and 13.3% cost saving values with the 3-hour and the extended tests, respectively. Even if the 17.5% cost decrease is significant for such kind of laboratory rig, the large influence of the demand curves cannot allow to evaluate the maximum saving value. The influence of the historical data in the tool for the storage vessel management could be important in case of very different demand trends during subsequent periods. However, the extended tests demonstrated that in several cases this influence can be accepted because the demand variations during the presented test are perfectly sustainable by the real-time tool, as demonstrated by the 13.3% cost saving.

Table 3

Also in this case a sensitivity analysis was carried out considering the effect of different electricity prices. The main economic results are shown in Tab.3 considering the comparison between the standard management approach and the test carried out with the real-time tool (including the thermal storage vessel management). The results reported in Tab.3 show a significant economic benefit obtained with the tool in all unitary electrical cost conditions (fuel price was constant in all cases).

Table 4

To complete the cost sensitivity analysis Tab.4 shows the effect of different fuel prices considering countries with lower costs (in comparison with the Italian situation). For this analysis the electricity prices were maintained constant: 0.24 €/kWh for energy purchased from the grid and -0.11 €/kWh for the energy sold to the grid. Also in this case, the values show that significant marginal cost decrease is obtainable with the real-time tool (vessel management included) at low fuel price conditions.

7. Application in a real complex polygeneration grid

Since the real-time tool operating in connection with the thermal storage simplified model was implemented considering the application in a complex polygeneration grid, this section discusses the details related to this generation management.

A complex polygeneration grid is a system including hundreds or thousands of prime movers and thermal (and/or electrical) storage devices. While the generation is mainly involving electrical and heating thermal power, districts including cooling power in tri-generation mode can be considered. In this case, it is necessary to include the management of absorption chillers and the related connection with the heating thermal grid. The district equipped with the complex polygeneration grid is composed of buildings including different technology. While, in general, each building can be equipped with prime movers, end users and energy storage devices, in such a complex district different configurations are possible (e.g. buildings equipped with generators or with users only). Moreover, the prime movers can be operating in co-generation/tri-generation mode or based on a separated generation technology (e.g. photovoltaic panels). The integration of technologies based on fossil fuels with prime movers operating with renewable energy could be an essential aspect for future generation.

In such scenario, the optimization tool needs to be very complex, also considering the simplified approach presented in the paper. For instance, to evaluate the prime mover cost ranking, the tool has to receive the necessary field measurements (usually power and fuel mass flow rate) for each prime mover enabled to operate in the grid. The tool has to include a storage management subroutine (with the necessary input temperature measurements) for each energy storage device installed and operating in the district. Then, for each prime mover it is necessary to evaluate its set-point in real-time mode and the on/off status to reduce the generation marginal costs, considering the specific constraints (e.g. a temperature limit or a specific generation priority in case of renewable sources). This complexity justifies the development of simplified approaches for the management tool and for the vessel SoC calculation. However, as presented in the paper, the results could be considered reliable and effective considering the real-time performance necessary for these software technologies.

A further level of complexity is present in case the district is organized as a coupling of different sub-grids. In this case, each sub-grid has to be managed by a specific tool and an additional software (based on the same approach for the other tools) has to be included for the general district management (to allocate the demand values to each sub-grid reducing costs in comparison with the traditional management approach).

8. Conclusions

In this work three different models based on three different approaches (empirical, mathematical and physical) were developed to evaluate the state of charge in a hot water tank, which is able to act as a thermal storage device. Moreover, they were successfully compared with data obtained from the experimental facility [33] (100 kWe mGT, 20 kWe ICE, a thermal storage tank and fan coolers for thermal demand generation). In details, the following results were obtained:

- All the three storage models show a significant agreement for the SoC evaluation.
- Model n.2 (mathematical) shows a more discontinuous behaviour.
- Model n.3 (physical) shows a good agreement with Model n.1 (empirical) and seems to be the most reliable solution for its continuous trend.

Even if the complete physical approach is able to produce the most continuous SoC trend, the empirical model is an effective solution for applications requiring simple (low computational time) solutions due to the large number of components to be considered and the requirement of real-time performance.

Moreover, the experimental facility [33] was used to operate tests on polygeneration grid management, using a real-time tool equipped with the storage tank empirical model. This tool [27] is a simple management software, which was developed to decrease the marginal costs of complex grids (equipped with high number of generators and thermal storage tanks) during generation of both electrical and thermal energy. The main experimental results obtained from these tests are the following:

- The results obtained without the thermal storage tank management in the 3-hour test (this device was not excluded from the test rig, but it was simply maintained at fixed SoC set-point) showed a 10.2% marginal cost decrease in comparison with the standard machine management case (the ICE managed to satisfy its local thermal demand and the mGT operated on the rest of this thermal demand).

- The results obtained from the test carried out with the management of the thermal storage tank in the 3-hour test showed a further 8.1% marginal cost saving in comparison with the previous case.
- The results obtained from the extended test showed a 13.3% marginal cost saving in comparison with the standard machine management case.
- The results demonstrated the effective performance of this management tool (simple management algorithm equipped with a simple SoC calculation model), especially for the management of complex grids where complex modelling and optimization techniques could not be acceptable. For the SoC calculation through the empirical model, a comparison test with model n.3 was successfully carried out with the management tool (0.3% difference in total marginal costs).

Currently, this tool (with the empirical SoC calculation model for the thermal storage tank) is successfully operating to satisfy the real load demands of the University campus.

Acknowledgements

The authors would like to thank Mr. Zachary Santer, student from the West Virginia University (USA), for his contribution in the management tool development. Moreover, Mr. Alberto Nicola Traverso, Ph.D. student at TPG, deserves acknowledgment and appreciation for his efforts in the validation activities on the model n.3 for the storage tank.

Nomenclature

Variables

A	section [m^2]
a, b, c, d, e	coefficients
E	energy [J]

H	enthalpy [J]
m	mass [kg]
N	number of calculation sections
P	power [W]
q	heat flux [W]
SoC	State of Charge [%]
T	temperature [°C]
t	time [s]
v	speed [m/s]
z	storage vessel height [m]
ρ	density [kg/m^3]

<u>Subscripts</u>

1, 2, 3, 4	temperature probe number
c	conduction
conv	convection
dem	demand
el	electrical
gen	generation
i	node number
ICE	Internal Combustion Engine
m	mass flow
M1	Model n.1 for SoC calculation
M3	Model n.3 for SoC calculation
max	maximum
mGT	micro Gas Turbine
s	stratification

Sto	Storage
tot	total
th	thermal

Acronyms

ICE	Internal Combustion Engine
mGT	micro Gas Turbine
Std	Standard
Sto	Storage
TPG	Thermochemical Power Group

References

[1] Zhang J., Liu P., Zhou Z., Ma L., Li Z., Ni W., A mixed-integer nonlinear programming approach to the optimal design of heat network in a polygeneration energy system. Applied Energy 114 (2014) 146-154.

[2] El-khattam W., Distributed Generation Technologies, definitions and benefits. Electric Power Systems Research 71 (2004) 109-121.

[3] Nojavan S., Zare K., Mohammadi-Ivatloo B., Optimal stochastic energy management of retailer based on selling price determination under smart grid environment in the presence of demand response program. Applied Energy 187 (2017) 449-46.

[4] Keshtkar A., Arzanpour S., An adaptive fuzzy logic system for residential energy management in smart grid environments. Applied Energy 186 (2017) 68-81.

[5] Fan C., Xiao F., Wang S., Development of prediction models for next-day building energy consumption and peak power demand using data mining techniques. Applied Energy 127 (2014) 1-10.

[6] Yan J., Chou S.K., Desideri U., Xia X., Innovative and sustainable solutions of clean energy technologies and policies (Part I). Applied Energy 130 (2014) 447-449.

[7] Zidan A., El-Saadany E.F., Distribution system reconfiguration for energy loss reduction considering the variability of load and local renewable generation. Energy 59 (2013) 698-707.

[8] Wu J., Yan J., Jia H., Hatziargyriou N., Djilali N., Sun H., Integrated Energy Systems. Applied Energy 167 (2016) 155-157.

[9] Greco A., Sorce A., Littwin R., Costamagna P., Magistri L., Reformer faults in SOFC systems: Experimental and modeling analysis, and simulated fault maps. International Journal of Hydrogen Energy 39 (2014) 21700-21713.

[10] Ferrari M.L., Sorce A., Pascenti M., Massardo A. F., Recuperator dynamic performance: Experimental investigation with a micro gas turbine test rig", Applied Energy 88 (2011) 5090-5096.

[11] Ferrari M.L., Pascenti M., Magistri L., Massardo A.F., MGT/HTFC hybrid system emulator test rig: Experimental investigation on the anodic recirculation system. Journal of Fuel Cell Science and Technology 8 (2011) 021012 1-9.

[12] Wakui T., Kinoshita T., Yokoyama R., A mixed-integer linear programming approach for cogeneration-based residential energy supply networks with power and heat interchanges, Energy 68 (2014) 29-46.

[13] Lin S.-Y., Chen J.-F., Distributed optimal power flow for smart grid transmission system with renewable energy sources, Energy 56 (2013) 184-192.

[14] Korkas C.D., Baldi S., Michailidis I., Kosmatopoulos E.B., Occupancy-based demand response and thermal comfort optimization in microgrids with renewable energy sources and energy storage. Applied Energy 163 (2016) 93-104.

[15] Wang H., Yin W., Abdollahi E., Lahdelma R., Jiao W., Occupancy-based demand response and thermal comfort optimization in microgrids with renewable energy sources and energy storage. Applied Energy 159 (2015) 401-421.

[16] Ferrari M.L., Rivarolo M., Massardo A.F., Hydrogen production system from photovoltaic panels: Experimental characterization and size optimization. Energy Conversion and Management 116 (2016) 194-202.

[17] Caresana F., Pelagalli L., Comodi G., Renzi M., Microturbogas cogeneration systems for distributed generation: Effects of ambient temperature on global performance and components' behavior. Applied Energy 124 (2014) 17–27.

[18] Ferrari M.L., Traverso A., Massardo A.F., 2016 Smart polygeneration grids: experimental performance curves of different prime movers. Applied Energy 162 (2016) 622–630.

[19] Anvari-Moghaddam A., Seifi A., Niknam T., Alizadeh-Pahlavani M.R., Multi-objective operation management of a renewable MG (micro-grid) with back-up micro-turbine/fuel cell/battery hybrid power source, Energy. 36 (2011) 6490-6507.

[20] Rong A., Lahdelma R., Role of polygeneration in sustainable energy system development challenges and opportunities from optimization viewpoints, Renewable and Sustainable Energy Reviews 53 (2016) 363-372.

[21] M. Gomez-Gonzalez, A. Lopez, F. Jurado, Optimization of distributed generation systems using a new discrete PSO and OPF, Electric Power Systems Research. 84 (2012) 174-180.

[22] Wang H., Abdollahi E., Lahdelma R., Jiao W., Zhou Z., Modelling and optimization of the smart hybrid renewable energy for communities (SHREC). Renewable Energy 84 (2015) 114-123.

[23] Sayedin F., Maroufmashat A., Sattari S., Elkamel A., Fowler M., Optimization of Photovoltaic Electrolyzer Hybrid systems; Taking into account the effect of climate conditions, Energy Conversion and Management 118 (2016) 438-449.

[24] Wang X., Palazoglu A., El-Farra N.H. Operational optimization and demand response of hybrid renewable energy systems. Applied Energy 143 (2015) 324-335.

[25] Ferrari M.L., 2015, Advanced control approach for hybrid systems based on solid oxide fuel cells. Applied Energy 145 (2015) 364-373.

[26] Fardadi M., McLarty D.F., Jabbari F., Investigation of thermal control for different SOFC flow geometries. Applied Energy, 178 (2016) 43-55.

[27] Ferrari M.L., Pascenti M., Sorce A., Traverso A., Massardo A.F., Real-time tool for management of smart polygeneration grids including thermal energy storage. Applied Energy 130 (2014) 670-678.

[28] Borges C.L.T., Cantarino E., Microgrids reliability evaluation with renewable distributed generation and storage systems, Proceedings of 18th IFAC world congress, session: grid expansion planning and operation considering renewable energy sources, 2011.

[29] Bellotti D., Rivarolo M., Magistri L., Massardo A.F., Thermo-economic comparison of hydrogen and hydro-methane produced from hydroelectric energy for land transportation. International Journal of Hydrogen Energy, 40 (2015) 2433-2444.

[30] Verda V., Colella F., Primary energy savings through thermal storage in district heating networks. Energy 36 (2011) 4278-4286.

[31] Kleinbach E.M., Beckman W.A., Klein S.A., Performance study of one-dimensional models for stratified thermal storage tanks. Solar energy 50 (1993) 155-166.

[32] Ihm P., Krarti M., Henze G.P., Development of a thermal energy storage model for EnergyPlus. Energy and Buildings 36 (2004) 807–814.

[33] Ferrari M.L., Traverso A., Pascenti M., Massardo A.F., Plant Management Tools Tested With a Small-Scale Distributed Generation Laboratory. Energy Conversion and Management, 78 (2014) 105–113.

[34] Li P., Xu B., Han J., Yang Y., Verification of a model of thermal storage incorporated with an extended lumped capacitance method for various solid-fluid structural combinations. Solar Energy, 105 (2014) 71-81.

[35] Lee K.S., A review on concepts, applications, and models of aquifer thermal energy storage systems. Energies, 3 (2010) 1320-1334.

[36] Kronhardt V., Alexopoulos S., Reißel M., Sattler J., Hoffschmidt B., Hänel M., Doerbeck T., High-temperature thermal storage system for solar tower power plants with open-volumetric air receiver simulation and energy balancing of a discretized model. Energy Procedia, 49 (2013) 870-877.

[37] Ghigliazza F., Traverso A., Massardo A.F., Wingate J., Ferrari M.L., Generic Real-Time Modeling of Solid Oxide Fuel Cell Hybrid Systems. Journal of Fuel Cell Science and Technology, 6 (2009) 021312_1-7.

[38] http://zone.ni.com/reference/en-XX/help/371361J-01/gmath/con_nonlin_curve_fit/, last access 06/09/2016.

[39] Negro F., 2013, Thermal storage for an energy-hub: model and experimental validation, Graduation Thesis (in Italian).

[40] http://ec.europa.eu/eurostat/statistics-explained/images/5/52/Half-yearly_gas_prices_%28in_EUR%29.png, last access 06/09/2016.

[41] http://ec.europa.eu/eurostat/statistics-explained/images/2/29/Electricity_and_gas_prices%2C_second_half_of_year%2C_2013%E2%80%9315_%28EUR_per_kWh%29_YB16.png, last access 06/09/2016.

Figures

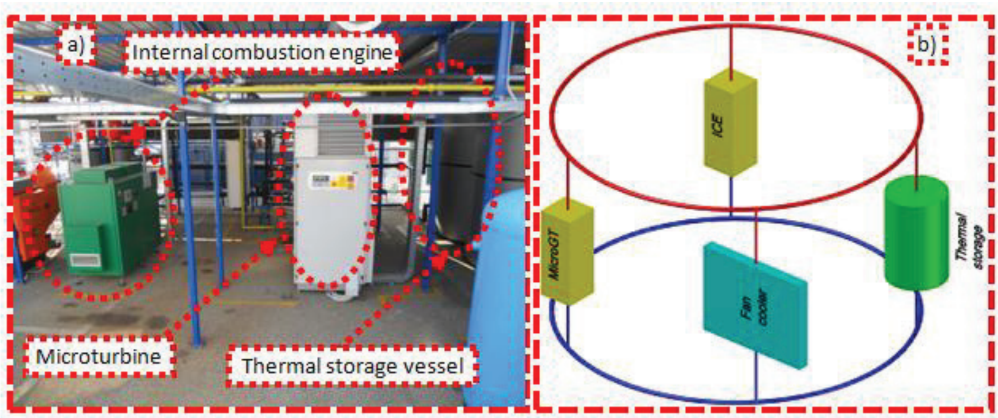

Figure 1. Laboratory test rig (a) and thermal grid layout (b).

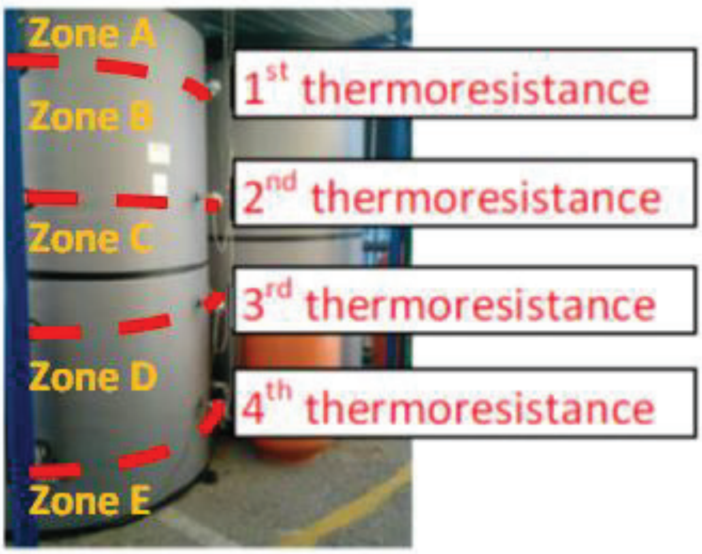

Figure 2. Stratification and thermoresistance scheme inside the thermal storage tank.

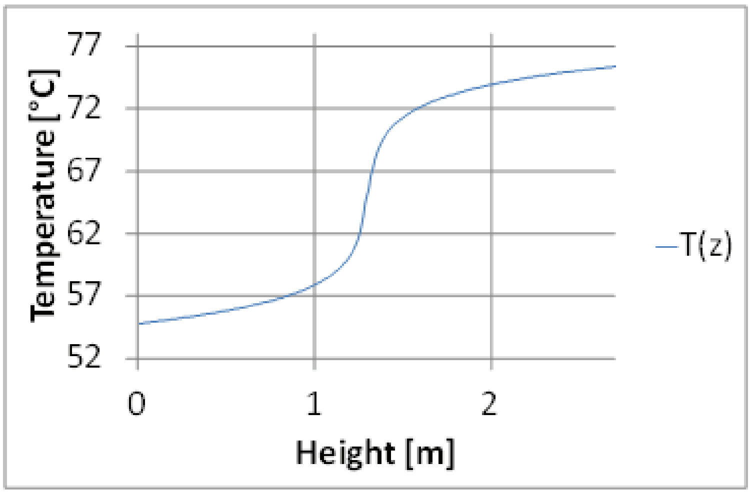

Figure 3. Example of temperature trend as a function of tank height for model n.3.

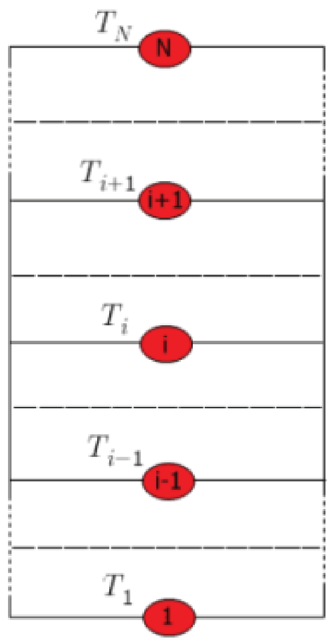

Figure 4. Discretization of a stratified water tank.

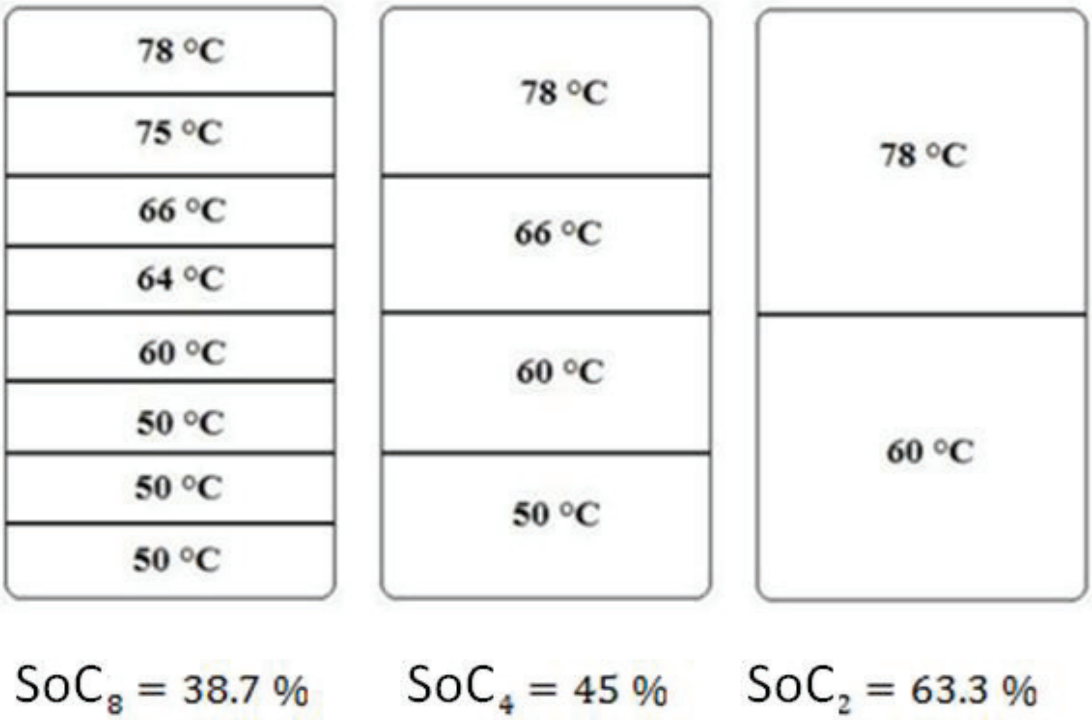

Figure 5. State of charge values calculated with different number of temperatures (different number of nodes).

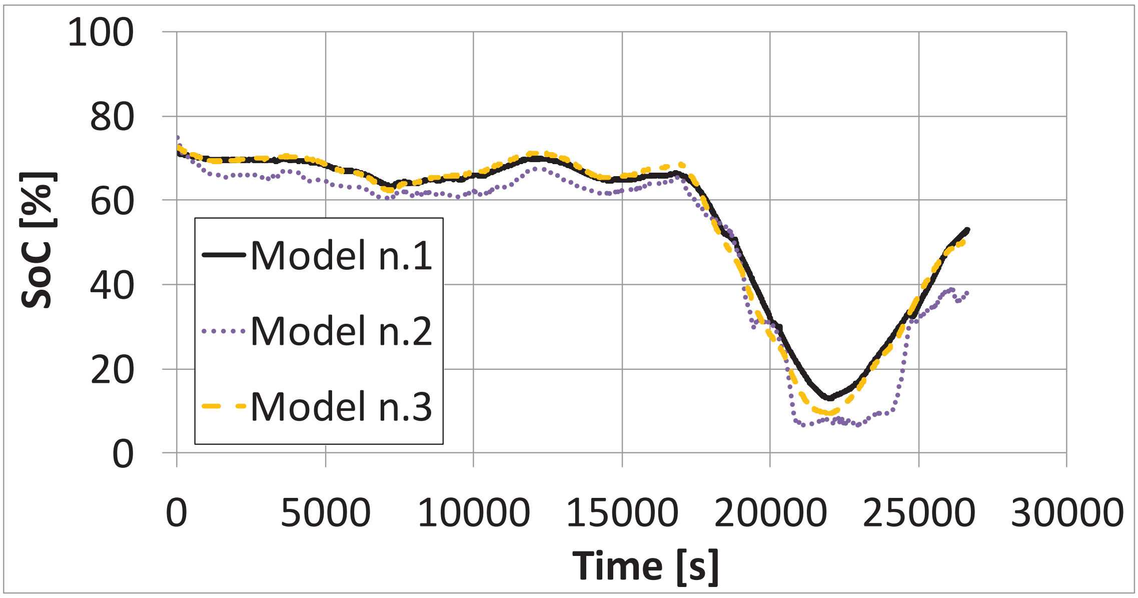

Figure 6. Model comparison (thermal storage state of charge).

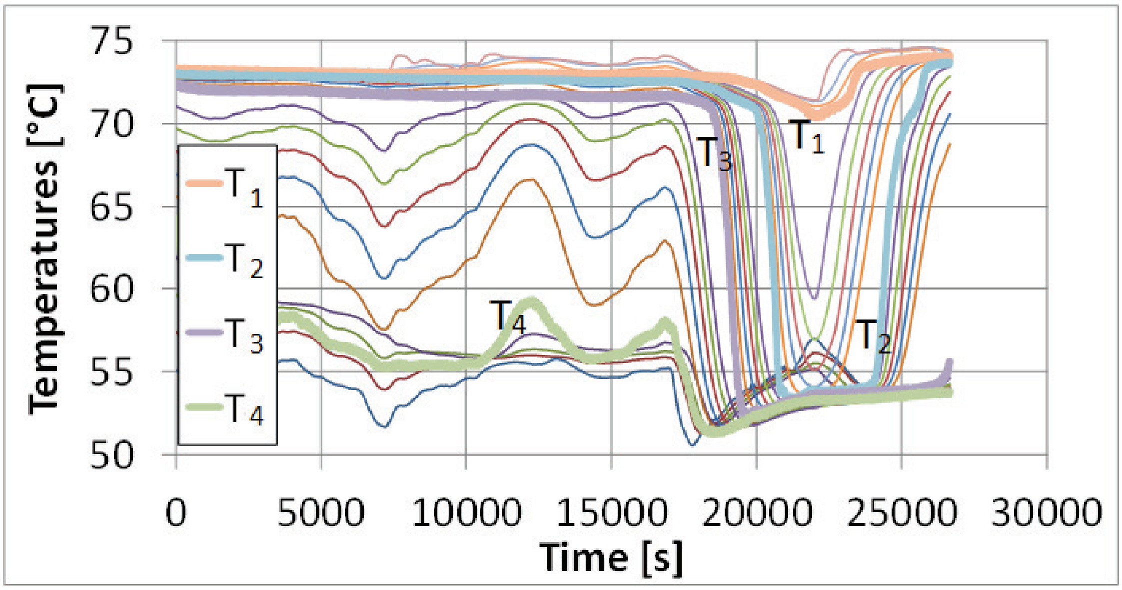

Figure 7. Temperature distribution: measured data (T_1, T_2, T_3 and T_4) and results obtained with the Model n.3.

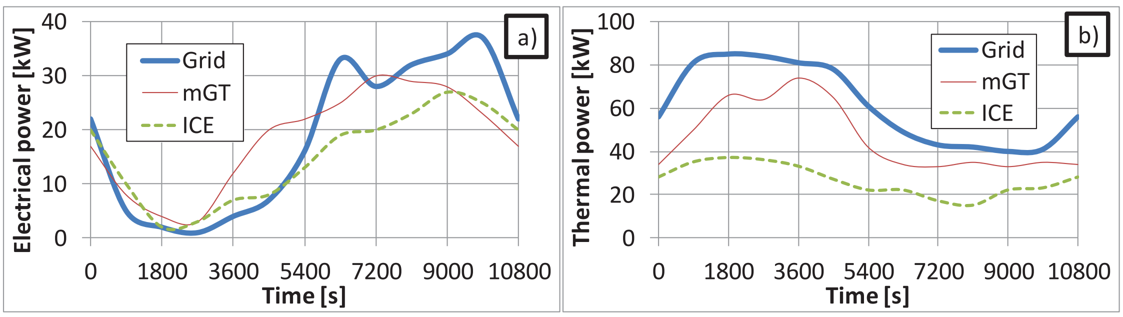

Figure 8. Electrical (a) and thermal (b) demand values used for the 3-hour grid management tests.

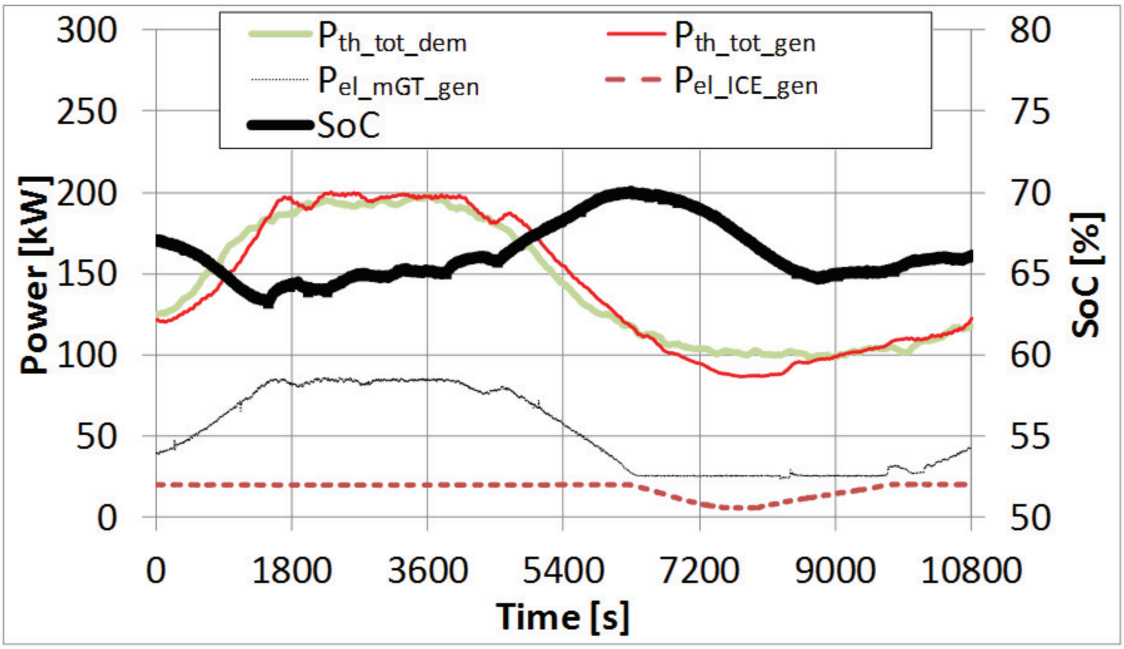

Figure 9. 3-hour grid management test without the management of the thermal storage tank: electrical, thermal powers and state of charge.

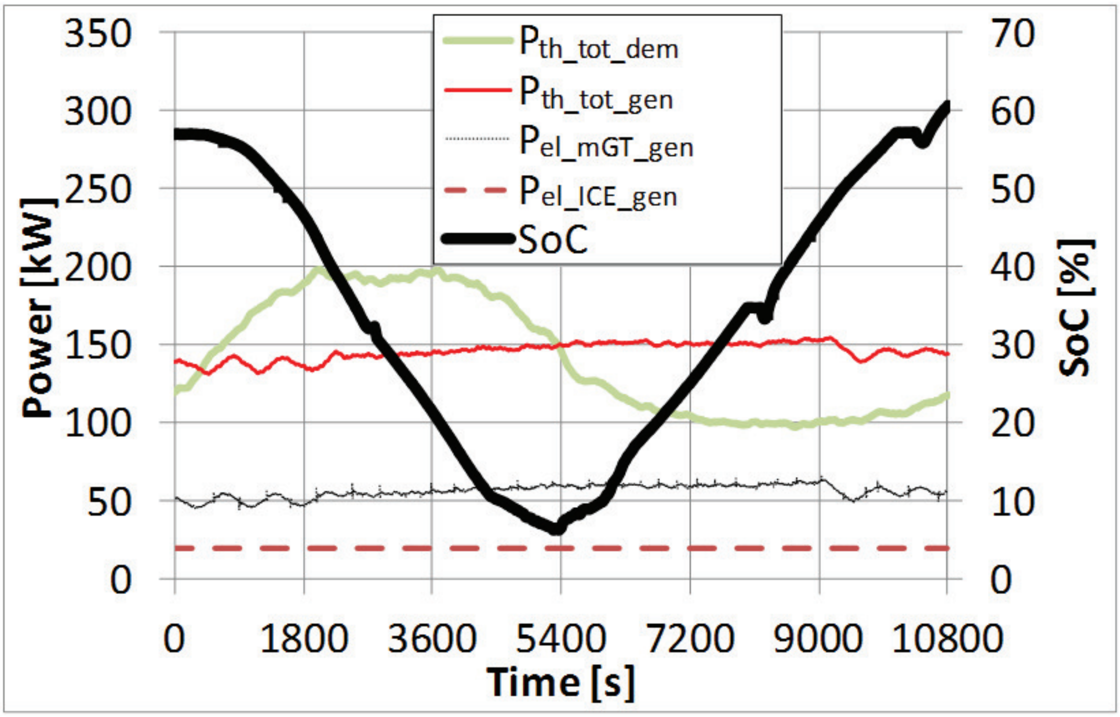

Figure 10. 3-hour grid management test with the management of the thermal storage tank: electrical, thermal powers and state of charge.

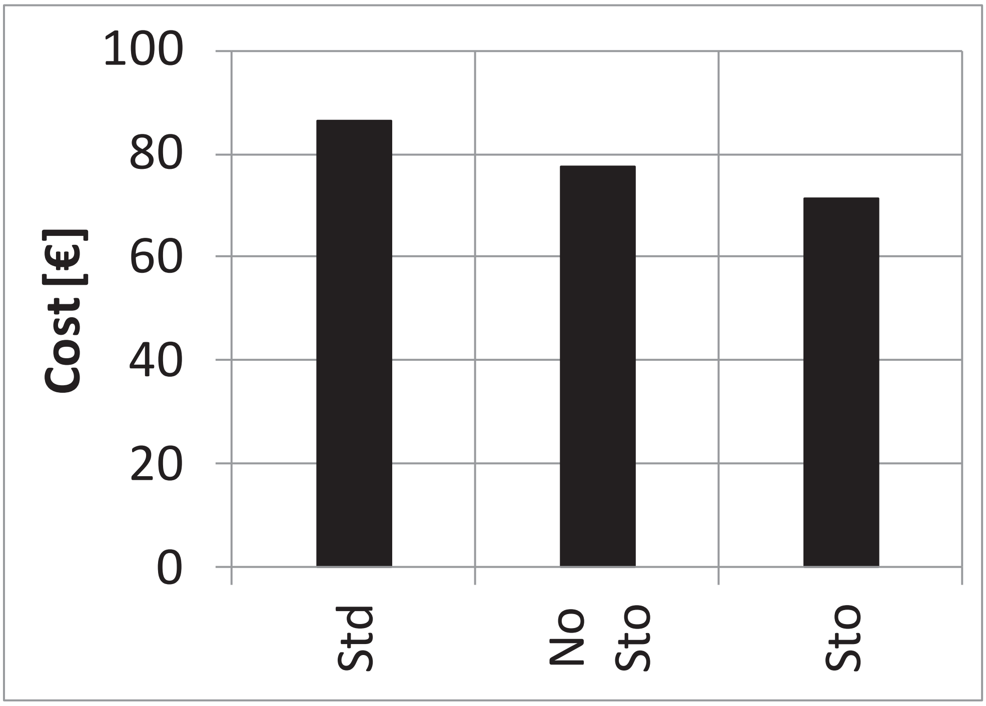

Figure 11. 3-hour grid management tests: comparison in terms of total marginal costs.

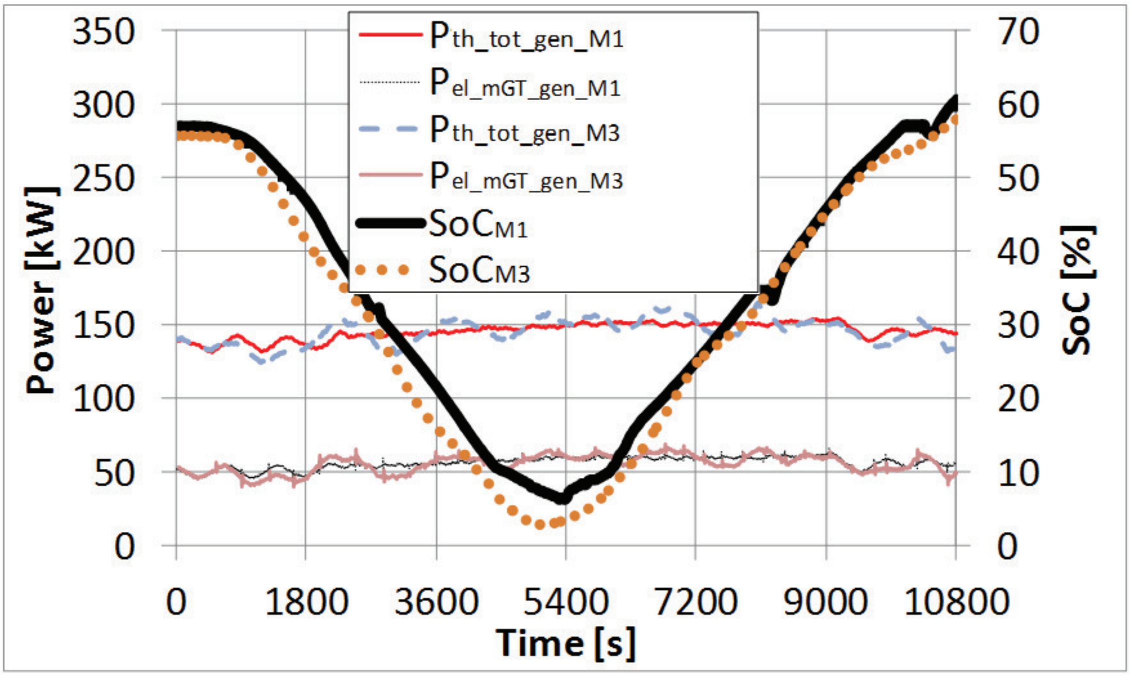

Figure 12. 3-hour grid management test with the management of the thermal storage tank: comparison of different SoC models.

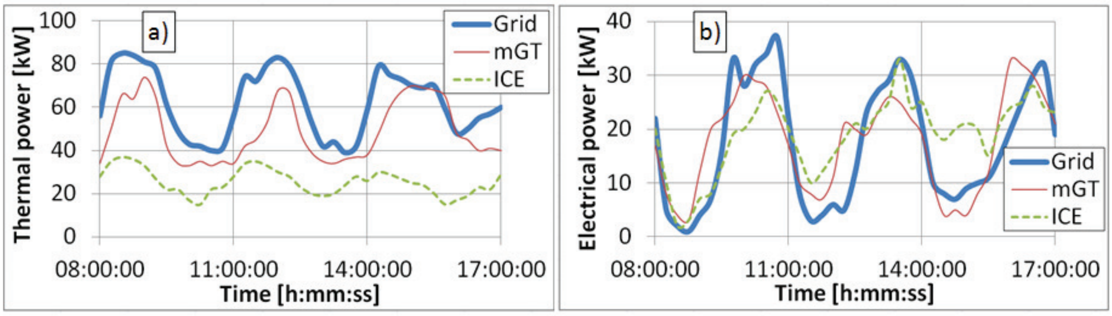

Figure 13. Electrical (a) and thermal (b) demand values used for the grid management in the extended test.

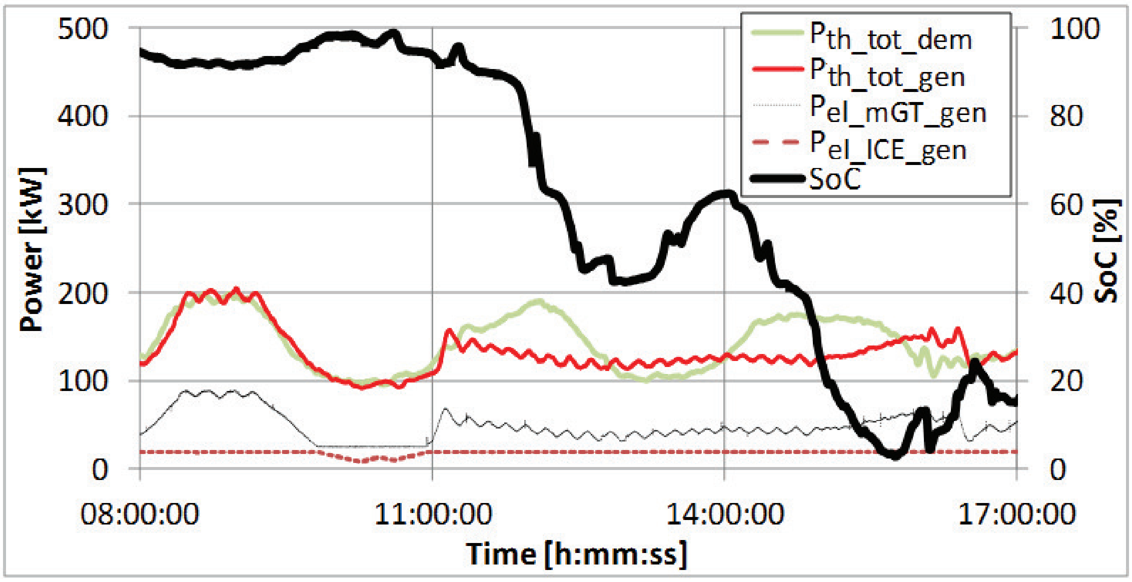

Figure 14. Extended test: electrical, thermal powers and storage state of charge.

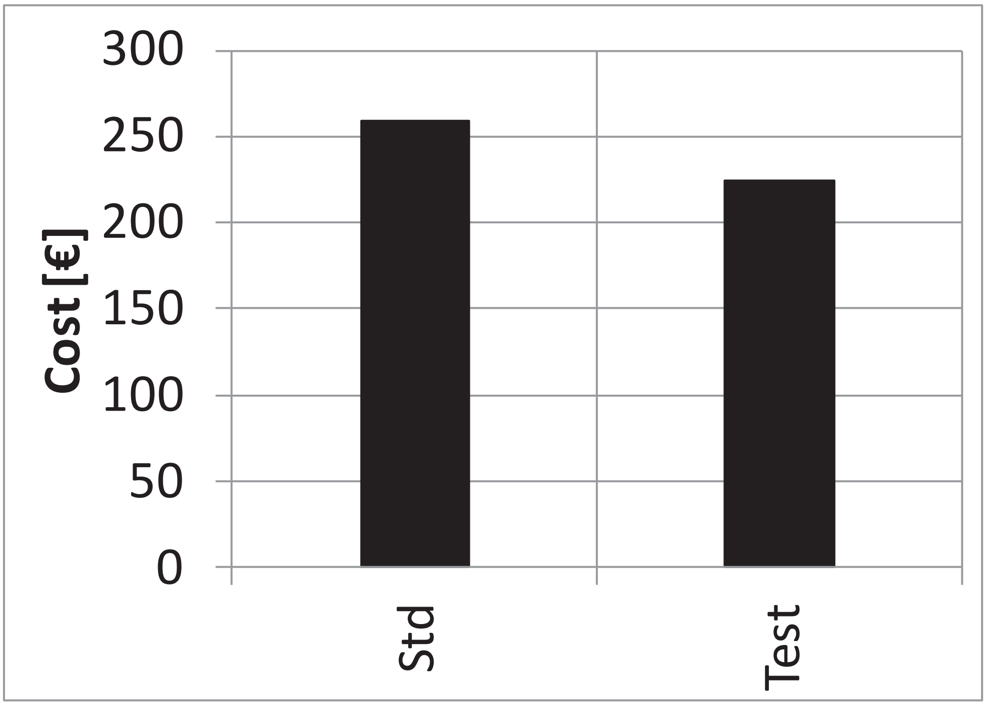

Figure 15. Extended test: comparison with the standard management case in terms of total marginal costs.